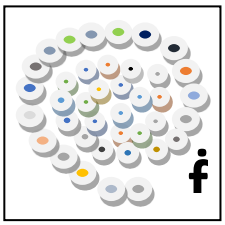

International Journal of Mathematical Analysis and Modelling

(Formerly Journal of the Nigerian Society for Mathematical Biology)

Volume 6, Issue 2 (Oct.-Nov.), 2023

ISSN (Print): 2682 - 5694
ISSN (Online): 2682 - 5708

International Journal of Mathematical Analysis and Modelling
Volume 6, Issue 2, October-November 2023, pages 1 - 12

Mathematical modeling of two-dimensional size exclusion chromatography model comparing fully porous and core-shell particles

U.D. Uche*†, A.O. Salaudeen‡, N.F. Okechi§ and A.G. Ahmad¶

Abstract

This work presents a comparison of fully porous and core-shell particles for size-exclusion chromatography. A two-dimensional general rate model is formulated for a column of cylindrical geometry. The model equations consist of a system of partial differential equations. Semi-analytical solutions are obtained for the formulated model equations by applying Hankel and Laplace transformations one after the other. This task is aimed at theoretically investigating and comparing the separation process output for both fully porous and core-shell particles for size-exclusion chromatography operations under isothermal conditions. The simulations in this work are used to demonstrate the size-exclusion effect for fully porous and core-shell particles and the results show better resolution of elution profiles are obtainable for some range of values of core radius fraction.

Keywords: general rate model; core-shell particles; semi-analytical solutions; size-exclusion chromatography

1 Introduction

Size-exclusion chromatography (SEC) is a versatile and widely used chromatographic technique (10). It operates on the principle of separating macromolecules based on their size (19). SEC utilizes a porous stationary phase (such as gel or resin) through which the sample is passed (10). Smaller molecules, which can penetrate the pores, take longer to elute, while larger molecules elute faster (10). SEC is commonly used for the analysis of macromolecules like proteins, nucleic acids, and synthetic polymers (10). It offers advantages such as simplicity, high resolution, and mild separation conditions (19). SEC has applications in various scientific disciplines, including biochemistry, biotechnology, polymer chemistry, and pharmaceutical analysis (10). It aids in determining the molar mass averages and distributions of macromolecules (24). This technique is commonly used in two-dimensional separations to determine the molar mass and chemical composition distributions of a sample (24).

A wide application of SEC can be found in several reports in the literature (1; 4; 5; 8; 17; 18; 22; 23; 24; 25; 26; 27; 28). However, practitioners must be aware of some of the pitfalls and challenges associated with SEC which include low feed volume to column volume ratio (24; 29). Despite these challenges, SEC remains an important technique as Luo and co-researchers compared the use of fully porous beads and cored beads in SEC for protein purification (16). The adsorption of poly(maleic) acid, natural organic matter and humic acid from river water on activated carbon was studied using SEC by (12). They measured the molecular weight distribution of polyelectrolytes remaining in the solution after equilibrium with activated carbon. Kaczmarski and co-workers used SEC to evaluate

*Corresponding Author. E-mail: uuche@nmc.edu.ng, duj_uche@yahoo.com
†Mathematics Programme, National Mathematical Centre Abuja, Nigeria; Department of Mathematics, University of Abuja, Nigeria
‡Department of Applied Mathematics (Chemistry Unit), National Mathematical Centre Abuja, Nigeria
§Mathematics Programme, National Mathematical Centre Abuja, Nigeria
¶Department of Applied Mathematics, Federal University of Technology, Babura, Jigawa State, Nigeria

competitive adsorption of a non-ionic surfactant and non-ionic hydrophobe-modified ethoxylated urethane thickener on pre-treated rutile titanium dioxide pigments (11).

Core-shell particles, also known as fused-core, solid core, or superficially porous particles, have been widely used in liquid chromatography, particularly in high-performance liquid chromatography (HPLC) (9). These particles consist of a solid core and a porous shell, which allows for efficient and fast separation with low operating pressure (9). They are prepared using various methods and offer advantages such as low back pressure and improved performance compared to other types of silica particles (9). Core-shell particles are commonly used in reversed-phase HPLC, where they have been found to reduce the plate height by up to 1.7 times (20). Their applications in liquid chromatography are diverse and continue to be explored for further advancements in the field (9).

Several mathematical models have been suggested to describe the size exclusion chromatography (13; 14; 15; 30). These models are very useful as they eliminate the risks involved in experimental processes. A two-dimensional general rate model in which the stationary phase equation is similar to the one-dimensional model implemented by Luo et al is applied in this work (16). To the best of the knowledge of the authors, there are no reported theoretical study carried out on SEC applied a two-dimensional general rate model comparing fully porous and core-shell particles.

The use of the two-dimensional model is very important in SEC as it captures the effects of radial disturbances at the point of solutes injection into the column. This phenomenon may occur in reality for large column operations, which is a significant feature of industrial SEC separations. The model equation consists of a system of partial differential equations and closed with typical initial and the Danckwerts boundary conditions. Semi-analytical solutions are obtained by applying Hankel and Laplace transformations one after the other (2; 21). The solutions are termed semi-analytical because the process of obtaining them involves a combination of both analytical and numerical procedures.

SEC is an industrial operation that involves very large columns and modeling this process mathematically is adequately captured using a two-dimensional model equation. The main objective of this work is to theoretically compare the separation processes involving the use of fully porous particles and core-shell particles under isothermal operating conditions. To achieve this, the following are carried out:

- formulate a two-dimensional general rate model for a cylindrical column packed with core-shell particles used to simulate SEC process operating under isothermal condition.
- define appropriate initial and boundary conditions for the system of equations.
- obtain semi-analytical solutions of the model equations by applying Hankel and Laplace transforms one after the other.
- determine the performance of the chromatographic column by comparing profile outputs of fully porous particles with that obtained for core-shell particles.

2 Mathematical model

The following assumptions are made to obtain the governing equations of the system:

- the column is operated under an isothermal condition
- both radial and axial transport of solute is considered
- given t as time, solute travels along the radial coordinate r by means of dispersion and along the axial coordinate z by means of advection with a constant velocity throughout the length of the column; and by means of dispersion
- the cylindrical column has radius R_{c}, packed with uniform sized spherically shaped particles of radius R_{p}

- there is no interaction between the solutes inside the column
- the column is designed such that solute can be injected via an inner region or an outer region; and as a consequence, a new parameter $\bar{r}$ is introduced, see Figure 1
- lastly, only injection of solutes through the inner region are considered

Given the above assumptions, the governing equations of the model representing the bulk and particle phases are given as

$$\frac{\partial c_{\mathrm{b}}}{\partial t}+u\frac{\partial c_{\mathrm{b}}}{\partial z}-D_{\mathrm{z}}\frac{\partial^2 c_{\mathrm{b}}}{\partial z^2}-D_{\mathrm{r}}\left(\frac{\partial^2 c_{\mathrm{b}}}{\partial r^2}+\frac{1}{r}\frac{\partial c_{\mathrm{b}}}{\partial r}\right)+F_{\mathrm{b}}\frac{3}{R_{\mathrm{p}}}k_{\mathrm{ext}}\left(c_{\mathrm{b}}-c_{\mathrm{p}}|_{r_{\mathrm{p}}=R_{\mathrm{p}}}\right)=0, \tag{1}$$

$$\epsilon_{\mathrm{p}}^{a}\frac{\partial c_{\mathrm{p}}}{\partial t}-\epsilon_{\mathrm{p}}^{a}D_{\mathrm{p}}\left(\frac{\partial^2 c_{\mathrm{p}}}{\partial r_{\mathrm{p}}^2}+\frac{2}{r_{\mathrm{p}}}\frac{\partial c_{\mathrm{p}}}{\partial r_{\mathrm{p}}}\right)=0. \tag{2}$$

In the above equations, u is the interstitial velocity, $F_{\mathrm{b}}=\frac{(1-\epsilon_{\mathrm{b}})}{\epsilon_{\mathrm{b}}}$, where ϵ_{b} is known as the external porosity and ϵ_{p} is called the internal particle porosity. D_{zi}, D_{ri} and $D_{\mathrm{p}i}$ are the dispersion constants for axial, radial and particle coordinates respectively. In SEC modeling, a key parameter proposed by Gu

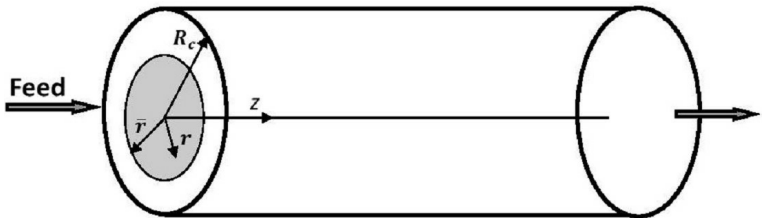

Figure 1: Schematic diagram of a chromatographic column of cylindrical geometry.

in (6) is the accessible porosity $\epsilon_{\mathrm{p}}^{a}$. For a very small molecule, $\epsilon_{\mathrm{p}}^{a}=\epsilon_{\mathrm{p}}$, because the particle macropores can be penetrated by the small molecule. For medium sized molecules, $0<\epsilon_{\mathrm{p}}^{a}<\epsilon_{\mathrm{p}}$, and for large molecules, such that there is complete exclusion from the particle macropores, $\epsilon_{\mathrm{p}}^{a}=0$.

The above coupled system of partial differential equations (PDEs) can be nondimensionalized using the following dimensionless parameters:

$$x=\frac{z}{L},\quad \tau=\frac{ut}{L},\quad \rho=\frac{r}{R_{\mathrm{c}}},\quad \rho_{\mathrm{p}}=\frac{r_{\mathrm{p}}}{R_{\mathrm{p}}},\quad Pe_{\mathrm{z}}=\frac{Lu}{D_{\mathrm{z}}},\quad Pe_{\rho}=\frac{R_{\mathrm{c}}^2 u}{D_{\mathrm{r}}L},$$

$$\zeta=\frac{k_{\mathrm{ext}}R_{\mathrm{p}}}{\epsilon_{\mathrm{p}}^{a}D_{\mathrm{p}}}\quad \eta=\frac{\epsilon_{\mathrm{p}}^{a}D_{\mathrm{P}}L}{R_{\mathrm{p}}^2 u},\quad \xi=3\zeta\eta F_{\mathrm{b}}.$$

Hence, equations (1) and (2) become:

$$\frac{\partial c_{\mathrm{b}}}{\partial \tau}+\frac{\partial c_{\mathrm{b}}}{\partial x}-\frac{1}{Pe_{\mathrm{z}}}\frac{\partial^2 c_{\mathrm{b}}}{\partial x^2}-\frac{1}{Pe_{\rho}}\left(\frac{\partial^2 c_{\mathrm{b}}}{\partial \rho^2}+\frac{1}{\rho}\frac{\partial c_{\mathrm{b}}}{\partial \rho}\right)+\xi\left[c_{\mathrm{b}}-c_{\mathrm{p}}|_{\rho_{\mathrm{p}}=1}\right]=0, \tag{3}$$

$$\epsilon_{\mathrm{p}}^{a}\frac{\partial c_{\mathrm{p}}}{\partial \tau}-\eta\left(\frac{\partial^2 c_{\mathrm{p}}}{\partial \rho_{\mathrm{p}}^2}+\frac{2}{\rho_{\mathrm{p}}}\frac{\partial c_{\mathrm{p}}}{\partial \rho_{\mathrm{p}}}\right)=0. \tag{4}$$

By following the procedure suggested by Gu in (6), for fully porous particles ρ_p ranges from 0 to 1, while for core-shell particles it ranges from $\rho_{\mathrm{core}}=R_{\mathrm{core}}/R_p$ to 1. Figure 1 shows a sketch of a spherical core-shell particle, with core radius fraction $\rho_{\mathrm{core}}=R_{\mathrm{core}}/R_p$. Thus, for arbitrary core radius fraction $\rho_{\mathrm{core}}\neq 0$, $\rho_{\mathrm{core}}\leq\rho_p\leq 1$ for core-shell particles. While for fully porous particles, ρ_{core}=0. We proceed to replace the ρ_p-axis by $0\leq\gamma\leq 1$, where the dimensionless radial axis is

$$\gamma=\frac{\rho_p-\rho_{\mathrm{core}}}{1-\rho_{\mathrm{core}}}\qquad\Rightarrow\qquad \rho_p=\gamma(1-\rho_{\mathrm{core}})+\rho_{\mathrm{core}}. \tag{5}$$

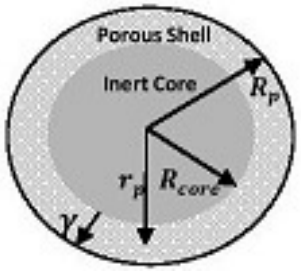

Figure 2: Schematic diagram of a core-shell particle.

For a column packed with core-shell particles, the governing equations are now obtained by substituting the above Eq.(5) into Eqs. (3) and (4) to obtain

$$\frac{\partial c_{\mathrm{b}}}{\partial \tau}+\frac{\partial c_{\mathrm{b}}}{\partial x}-\frac{1}{Pe_{\mathrm{z}}}\frac{\partial^2 c_{\mathrm{b}}}{\partial x^2}-\frac{1}{Pe_{\rho}}\left(\frac{\partial^2 c_{\mathrm{b}}}{\partial \rho^2}+\frac{1}{\rho}\frac{\partial c_{\mathrm{b}}}{\partial \rho}\right)+\xi\left[c_{\mathrm{b}}-c_{\mathrm{p}}|_{\gamma=1}\right]=0, \tag{6}$$

$$\epsilon_{\mathrm{p}}^{a}\frac{\partial c_{\mathrm{p}}}{\partial \tau}-\frac{\eta}{(1-\rho_{\mathrm{core}})^2}\left(\frac{\partial^2 c_{\mathrm{p}}}{\partial \gamma^2}+\frac{2(1-\rho_{\mathrm{core}})}{(\gamma(1-\rho_{\mathrm{core}})+\rho_{\mathrm{core}})}\frac{\partial c_{\mathrm{p}}}{\partial \gamma}\right)=0. \tag{7}$$

The system of PDEs require the following initial and boundary conditions.

Initial conditions:

$$c_{\mathrm{b}}(\rho,x,\tau=0)=0,\quad 0\le\rho\le 1,\ \ 0\le x\le 1, \tag{8}$$

$$c_{\mathrm{p}}(\gamma,\rho,x,\tau=0)=0,\quad 0\le\gamma\le 1,\ \ 0\le\rho\le 1,\ \ 0\le x\le 1. \tag{9}$$

For the symmetry of the radial profile and impermeable wall of the column, the following boundary conditions are used for equation (6) at $\rho=0$ and $\rho=1$:

$$\frac{\partial c_{\mathrm{b}}(\rho=0,x,\tau)}{\partial \rho}=0\,,\qquad \frac{\partial c_{\mathrm{b}}(\rho=1,x,\tau)}{\partial \rho}=0. \tag{10}$$

At both column boundaries, the Danckwerts boundary conditions are used. For pulse injection through the inner region:

$$c_{\mathrm{b}}(\rho,x=0,\tau)-\frac{1}{Pe_{\mathrm{z}}}\frac{\partial c_{\mathrm{b}}(\rho,x=0,\tau)}{\partial x}=\begin{cases} c_{\mathrm{b}}^{\mathrm{inj}}\,, & \text{if } 0\le\rho\le\bar{\rho} \text{ and } 0\le\tau\le\tau_{\mathrm{inj}}\,,\\ 0\,, & \bar{\rho}<\rho\le 1 \text{ or } \tau>\tau_{\mathrm{inj}}\,.\end{cases} \tag{11}$$

where $c_{\mathrm{b}}^{\mathrm{inj}}$ is the injected concentration and τ_{inj} is the dimensionless time of injection. At the outlet of the column, the classic Neumann boundary conditions is applied:

$$\left.\frac{\partial c_{\mathrm{b}}(\rho,x,\tau)}{\partial x}\right|_{x=1}=0\,. \tag{12}$$

Lastly for the particle phase, equation (7), the following boundary conditions are used at $\gamma=0$ and $\gamma=1$ as

$$\left.\frac{\partial c_{\mathrm{p}}}{\partial \gamma}\right|_{\gamma=0}=0,\quad \left.\frac{\partial c_{\mathrm{p}}}{\partial \gamma}\right|_{\gamma=1}=(1-\rho_{\mathrm{core}})\zeta(c_{\mathrm{b}}-c_{\mathrm{p}}|_{\gamma=1}). \tag{13}$$

3 Obtaining semi-analytical solutions

To obtain analytical solutions, the Hankel and Laplace transforms are applied one after the other. This technique and solution procedure are similar to the one presented by by David et al in (2) and Qamar

et al in (21); hence the details are omitted here. The solution obtained after applying the Danckwerts boundary condition is given below as:

$$\bar{c}_H(x,\lambda_n,s) = \frac{\left[m_2 e^{m2+m_1 x} - m_1 e^{m1+m_2 x}\right]\left[\frac{F(\lambda_n)}{s}\left(1-e^{-s\tau_{\text{inj}}}\right)\right]}{m_2 e^{m_2}\left(1-\frac{m_1}{Pe_z}\right) - m_1 e^{m_1}\left(1-\frac{m_2}{Pe_z}\right)}. \tag{14}$$

Where

$$m_{1,2} = \frac{Pe_z}{2}\left(1 \pm \sqrt{1+\frac{4\phi(s,\lambda_n)}{Pe_z}}\right) \tag{15}$$

and m_1 is obtained by choosing the plus sign and m_2 by choosing the minus sign. Also,

$$F(\lambda_n) = \begin{cases} \frac{\bar{\rho}^2}{2}, & \text{if } \lambda_n = 0, \\ \frac{\bar{\rho}}{\lambda_n} J_1(\lambda_n \bar{\rho}), & \text{if } \lambda_n \neq 0, \end{cases} \tag{16}$$

with λ_n representing the parameter of the finite Hankel transform that can be estimated using the equation $\frac{dJ_0(\lambda_n)}{d\rho} = -J_1(\lambda_n) = 0$. Where, $J_0(.)$ is the zeroth order, and $J_1(.)$ is the first order Bessel functions of the first kind.

The analytical Laplace inversion of the above obtained solution is not currently achievable. The numerical inversion technique proposed by Durbin in (3) is used to get semi-analytical solutions in the actual time domain.

4 Simulation results

The parameters used in the simulation of the process are given in Table 1. These parameters fall within

Table 1: Values of parameters used in simulation.

Parameter	Symbol	Value
External porosity	ϵ_{b}	0.4
Internal porosity	ϵ_{p}	0.66
Accessible porosity	ϵ_{p}^{a}	0.5
Axial Peclet number	Pe_{z}	1500
Radial Peclet number	Pe_{ρ}	37.5
Dimensionless constant	η	2
Dimensionless constant	ζ	50
Injected concentration	$c_{\text{bi}}^{\text{inj}}$	1 mol/L
Time of injection	τ_{inj}	1.0

the range typically used in experimental studies of liquid chromatography (7). Where the parameters differ from what is given in Table 1, they are clearly stated. The results are plotted at the outlet of the column showing the dimensionless time of elution.

4.1 Effect of core radius fraction ρ_{core} on elution profiles

Figure 3 shows that the peak of the elution profile become sharper and with narrower tails, which implies shorter retention times as the value of ρ_{core} is increased. The reduced intraparticle diffusional mass-transfer distance caused the sharpness of the peak and a shorter time of elution. In chromatography operations, the resolution of peaks is improved by sharper peaks. However, if the retention times are too short, the overall range of retention times in an SEC chromatogram becomes too small to effectively resolve multiple peaks.

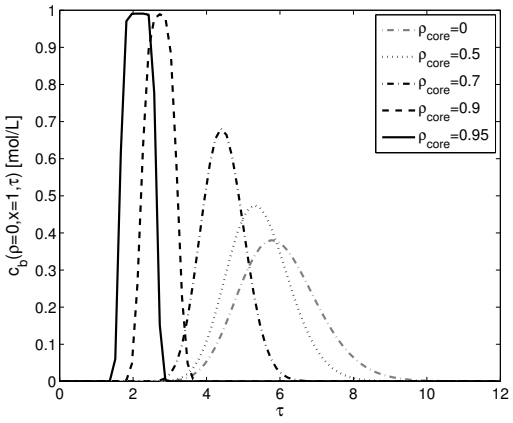

Figure 3: Effect of core radius fraction ρ_{core} on SEC

4.2 Effect of the accessible porosity parameter ϵ_p^a

The effect of the parameter ϵ_p^a is used to compare the results for both fully porous particles and core-shell particles. It can be seen in Figure 4 that for smaller values of ϵ_p^a, which implies small access for the molecules to penetrate the particles in the stationary phase, the elution is faster and thus resulting in shorter retention times. Although the retention times for both cases shown in Figure 4(a) can be said to be almost the same, significant increase in the retention times can be seen in Figures 4(b) to 4(d) as the value of ϵ_p^a is increased. A taller and narrower peak can be observed for the case where $\rho_{\text{core}} = 0.85$ compared to the fully porous particle case, that is where $\rho_{\text{core}} = 0$.

4.3 Effect of radial dispersion coefficient Pe_ρ

Under this subsection, $\rho_{\text{core}} = 0.6$ for the obtained results. Figure 5 shows that for smaller value of Pe_ρ, there is no gradient visible along the radial coordinate. This case reduces to a one-dimensional model. For increased Pe_ρ value, the evolution of gradients along the radial coordinate becomes evident. Thus, the radial disturbances in SEC operations is captured by the current two-dimensional model.

4.4 Effect of mass transfer parameters on band broadening and peak retention time

Again, $\rho_{\text{core}} = 0.6$ for the following results obtained here. In Figure 6(a), other parameters are fixed while Pe_{z} is altered to give the result shown. It can be seen that smaller values Pe_{z} cause a broader and tailing profile, which also leads to increased retention time. Similar phenomena are observed for the results for ζ and η as shown in Figures 6(b) and 6(c) respectively.

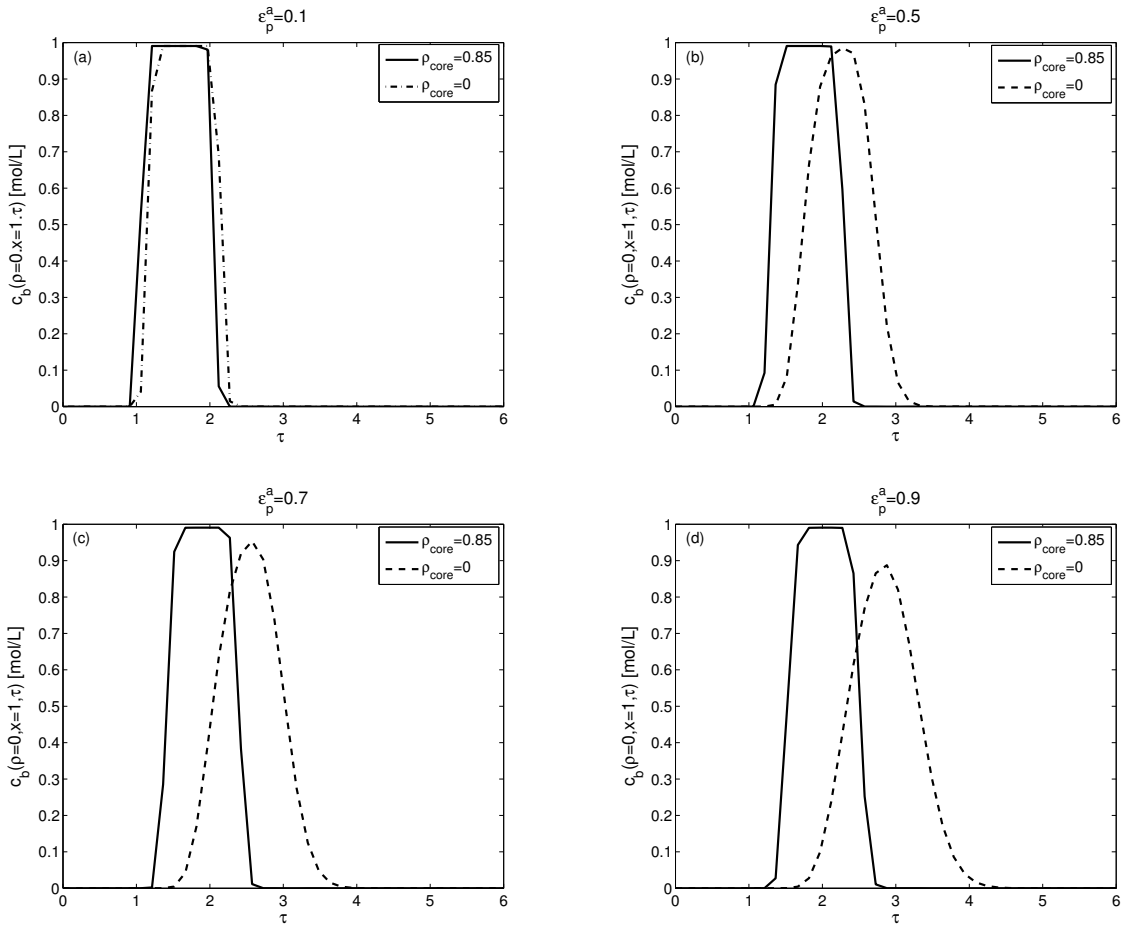

Figure 4: Size-exclusion effect for both fully porous particles and core-shell particles

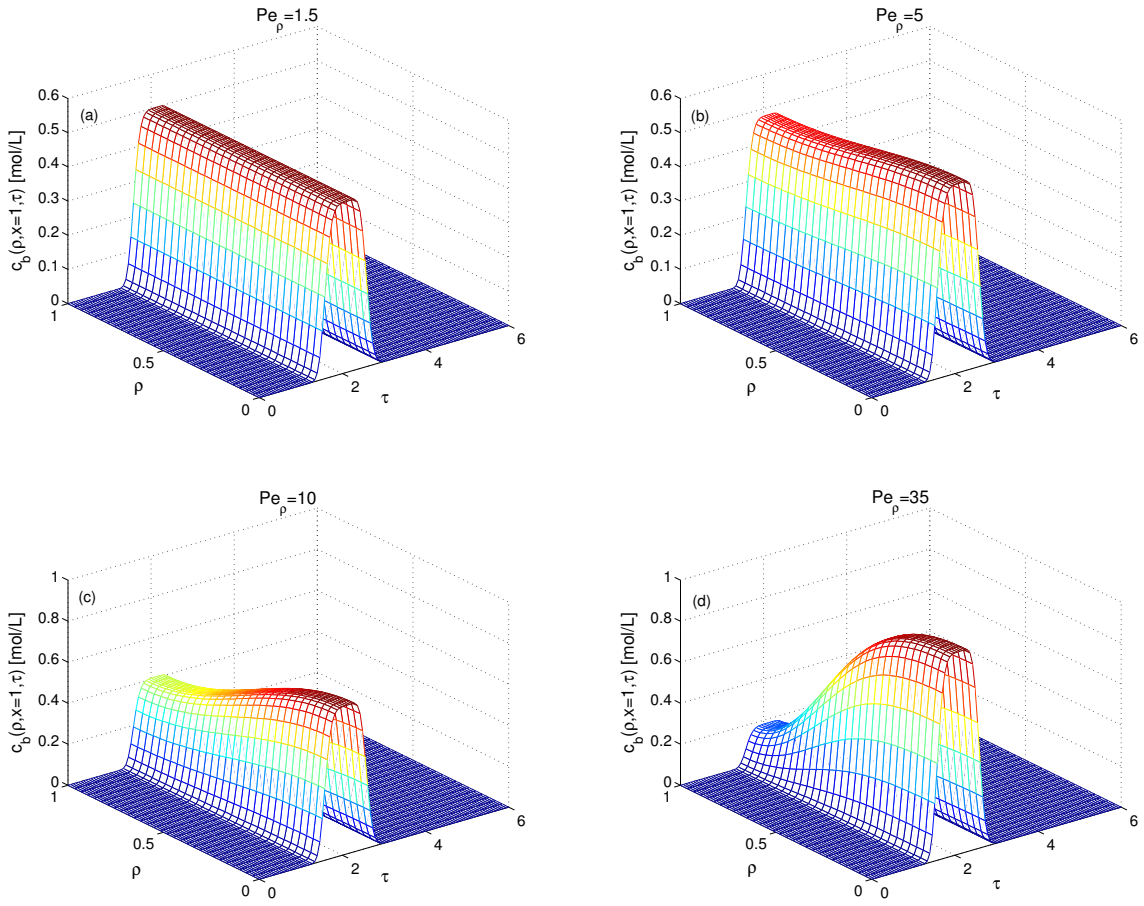

Figure 5: Effect of Pe_ρ on the elution profile

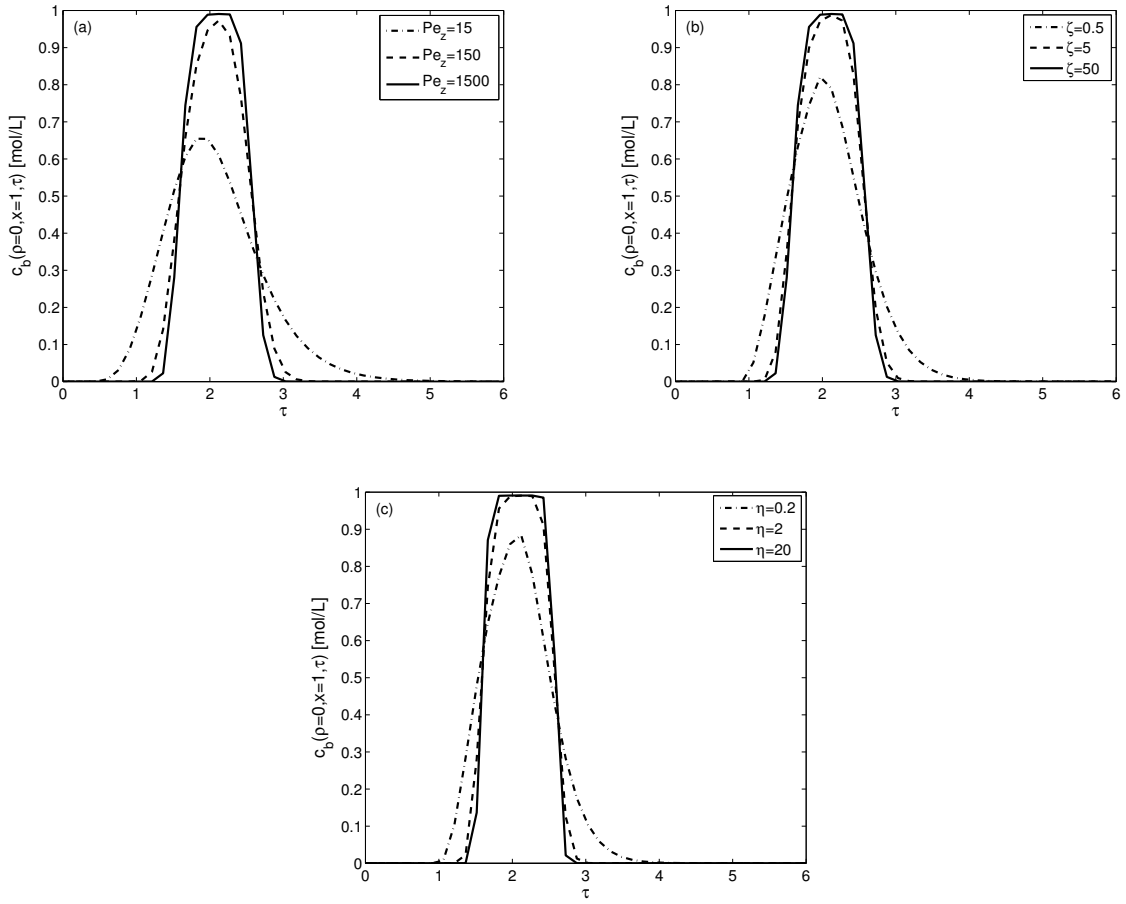

Figure 6: Effect of kinetic parameters Pe_z, ζ and η on the elution profiles

5 Conclusion

A two-dimensional general rate model was formulated and implemented to simulate size-exclusion chromatography process comparing fully porous and core-shell particles operation under isothermal conditions. Semi-analytical solutions of the formulated model equations were obtained by successively applying Hankel and Laplace transformations considering Danckwerts boundary condition. Despite the absence of any reported theoretical study on two-dimensional models, the larger column feature in SEC operations motivated its use in this study. The obtained results show that for some reasonable range of core radius fraction and accessible porosity values, better peak resolutions can be achieved in SEC processes.

References

[1] Barth, H. G., Boyes, B. E., Jackson, C., (1998). Size Exclusion Chromatography and Related Separation Techniques. Analytical Chemistry 70, 251R-278R.

[2] David, U. U., Qamar, S., Seidel-Morgenstern, A., (2018). Analytical and numerical solutions of two-dimensional general rate models for liquid chromatographic columns packed with core-shell particles, Chemical Engineering Research & Design 130, 295-320.

[3] Durbin, F., (1974). Numerical Inversion of Laplace Transforms: An efficient improvement to Dubner and Abate's Method. The Computer Journal 17, 371-376.

[4] Goyon, A., Fekete, S., Beck, A., Veuthey, J. -L., Guillarme, D., (2019). Unraveling the mysteries of modern size exclusion chromatography - the way to achieve confident characterization of therapeutic proteins. Journal of Chromatography B 1092, 368-378. https://doi.org/10.1016/j.jchromb.2018.06.029.

[5] Gritti, F., Hochstrasser, J., Svidrytski, A., Hlushkou, D., Tallarek, U., (2020). Morphology-transport relationships in liquid chromatography: Application to method development in size exclusion chromatography. Journal of Chromatography A 1620, 460991. https://doi.org/10.1016/j.chroma.2020.460991.

[6] Gu, T., (1995). Mathematical Modeling and Scale-Up of Liquid Chromatography. Springer, Berlin-New York.

[7] Guiochon, G., Felinger, A., Shirazi, D. G., Katti, A. M., (2006). Fundamentals of preparative and nonlinear chromatography, 2nd ed. ELsevier Academic press, New York.

[8] Guo, J., Wu, C., Lin, X., Zhou, J., Zhang, J., Zheng, W., Wang, T., Cui, Y., (2021). Establishment of a simplified dichotomic size-exclusion chromatography for isolating extracellular vesicles toward clinical applications. Journal of Extracellular Vesicles 10, e12145. https://doi.org/10.1002/jev2.12145.

[9] Hayes, R., Ahmed, A., Edge, T., Zhang, H., (2014). Core-shell particles: preparation, fundamentals and applications in high performance liquid chromatography. Journal of Chromatography A 29, 1357:36-52. doi: 10.1016/j.chroma.2014.05.010.

[10] Holbrook, R. D., Galyean, A. A., Gorham, J. M., Herzing, A., Pettibone, J., (2015). Chapter 2 - Overview of Nanomaterial Characterization and Metrology, Editor(s): Mohammed Baalousha, Jamie R. Lead, Frontiers of Nanoscience, Elsevier, Volume 8, Pages 47-87, ISSN 1876-2778, ISBN 9780080999487, https://doi.org/10.1016/B978-0-08-099948-7.00002-6.

[11] Kaczmarski, J.P., Tarng, M.R., Glassa, J. E., Buchacek, R. J., (1997). Development of and results from a chromatographic technique for the analysis of competitive adsorption on stabilized TiO_2 surfaces. Progress in Organic Coatings, 30(1-2):15-23.

[12] Kilduff, J.E., Karanfil, T., Chin, Y. -P., Weber, W. J., (1996). Adsorption of Natural Organic Polyelectrolytes by Activated Carbon: A Size-Exclusion Chromatography Study. Environmental Science & Technology, 30(4): 1336-1343.

[13] Kim, D. H., Johnson, J. A., (1984). Computer Model for Gel Permeation Chromatography of Polymers. 245. A.C.S. symposium series, ACS Publications, Washington, DC, pp. 25-45.

[14] Koo, Y. -M., Wankat, P. C., (1988). Modeling of size exclusion parametric pumping. Separation Science and Technology, 23:413-427.

[15] Li, Z., Gu, Y., Gu, T., (1998). Mathematical modeling and scale-up of size-exclusion chromatography. Biochemical engineering journal, 2:145-155.

[16] Luo, J., Zhou, W., Su, Z., Ma G., Gu, T., (2013). Comparison of fully-porous beads and cored beads in size exclusion chromatography for protein purification. Chemical Engineering Science, 102:99-105.

[17] Monguió-Tortajada, M., Morón-Font, M., Gámez-Valero, A., Carreras-Planella, L., Borràs, F.E., Franquesa, M., (2019). Extracellular-vesicle isolation from different biological fluids by size-exclusion chromatography. Current Protocols in Stem Cell Biology 49:e82. doi: 10.1002/cpsc.82.

[18] Monguiò-Tortajada, M., Gàlvez-Montòn, C., Bayes-Genis, A., Roura, S., Borràs, F. E., (2019). Extracellular vesicle isolation methods: rising impact of size-exclusion chromatography. Cellular and Molecular Life Sciences 76:2369-2382. https://doi.org/10.1007/s00018-019-03071-y

[19] Park, Y., Sillanpää, M., Anderson, L., Gagnon, G.A., Matilainen, A., (2023). Chapter 3 - Characterization of natural organic matter, Editor(s): Mika Sillanpää, Yuri Park, Natural Organic Matter in Water (Second Edition), Butterworth-Heinemann, Pages 43-92, ISBN 9780128242742, https://doi.org/10.1016/B978-0-12-824274-2.00002-8.

[20] Preti, R., (2016). Core-Shell Columns in High-Performance Liquid Chromatography: Food Analysis Applications. International Journal of Analytical Chemistry 3189724, https://doi.org/10.1155/2016/3189724.

[21] Qamar, S., Uche, D. U., Khan,F. U., Seidel-Morgenstern, A., (2017). Analysis of linear two-dimensional general rate model for chromatographic columns of cylindrical geometry. Journal of Chromatography A, 1496: 92-104.

[22] Rieder, A., Afseth, N. K., Böcker, U., Knutsen, S. V., Kirkhus, B., Mæhre, H. K., Ballance, S., Wubshet, S. G., (2021). Improved estimation of in vitro protein digestibility of different foods using size exclusion chromatography. Food Chemistry, 358:129830. https://doi.org/10.1016/j.foodchem.2021.129830.

[23] Some, D., Amartely, H., Tsadok, A., Lebendiker, M., (2019). Characterization of Proteins by Size-Exclusion Chromatography Coupled to Multi-Angle Light Scattering (SEC-MALS). Journal of Visualized Experiments, 148:59615. doi:10.3791/59615.

[24] Striegel, A. M., (2022). Size-Exclusion Chromatography: A Twenty-First Century Perspective. Chromatographia, 85:307-313. https://doi.org/10.1007/s10337-022-04143-1.

[25] Štulík, K., Pacáková, V., Tichá, M., (2003). Some potentialities and drawbacks of contemporary size-exclusion chromatography. Journal of Biochemical Biophysical Methods, 56:1-13.

[26] Süß, S., Metzger, C., Damm, C., Segets, D., Peukert, W., (2018). Quantitative evaluation of nanoparticle classification by size-exclusion chromatography. Powder Technology, 339:264-272. https://doi.org/10.1016/j.powtec.2018.08.008.

[27] Takov, K., Yellon, D. M., Davidson, S. M., (2019). Comparison of small extracellular vesicles isolated from plasma by ultracentrifugation or size-exclusion chromatography: yield, purity and functional potential. Journal of Extracellular Vesicles 8:1. DOI: 10.1080/20013078.2018.1560809.

[28] Ventouri, I. K., Malheiro, D. B. A., Voeten, R. L. C., Sander, K., Maarten, H., Govert W.S., Haselberg, R., (2020). Probing Protein Denaturation during Size-Exclusion Chromatography Using Native Mass Spectrometry. Analytical Chemistry 92 (6), 4292-4300. DOI: 10.1021/acs.analchem.9b04961.

[29] Wheelwright, S. M., (1994). Protein Purification: Design and Scale Up of Downstream Processing. Wiley, New York, NY, USA.

[30] Yau, W. W., Kirkland, J. J., Bly, D. D., (1979). Modern size-exclusion liquid chromatography. Wiley, New York, p 89.